analytical chemistry

Technical Note

pubs.acs.org/ac

# Electronic Detection of MicroRNA at Attomolar Level with High Specificity

Pankaj Ramnani,[‡,†] Yingning Gao,[‡,†] Mehmet Ozsoz,[§] and Ashok Mulchandani*[,‡]

[‡]Department of Chemical and Environmental Engineering, University of California, Riverside, California 92521, United States

[§]Department of Biomedical Engineering, Izmir Katip Celebi University, Cigli, Izmir, Turkey 35620

Supporting Information

**ABSTRACT:** Small RNA (19−23 nucleotides) molecules play an important role in gene regulation, embryonic differentiation, hematopoiesis, and a variety of cancers. Here, we present an ultrasensitive, extremely specific, label-free, and rapid electronic detection of microRNAs (miRNAs) using a carbon nanotubes field-effect transistor functionalized with the Carnation Italian ringspot virus p19 protein biosensor. miRNA-122a was chosen as the target, which was first hybridized to a probe molecule. The probe-miRNA duplex was then quantified by measuring the change in resistance of biosensor resulting from its binding to p19, which selects 21−23 bp RNA duplexes in a size-dependent but sequence-independent manner. The biosensor displayed a wide dynamic range up to $10^{-14}$ M and was able to detect as low as 1 aM miRNA in the presence of a million-fold excess of total RNA, paving the way for simple, point-of-care, low-cost early detection of miRNA as a biomarker in diagnosis of many diseases, including cancer.

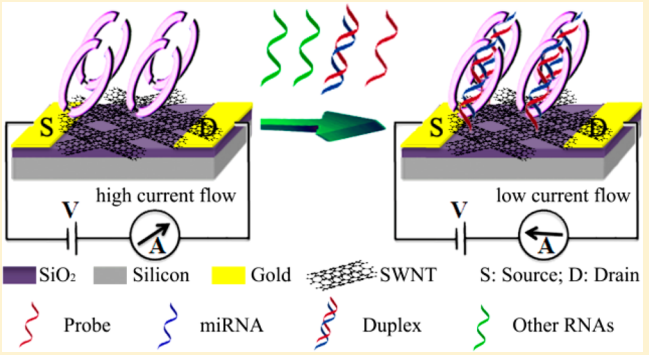


Since their discovery two decades ago, microRNAs (miRNAs) have emerged as a new modality in medical diagnostics. These small endogenous biomolecules of ∼22 nucleotides in length have been linked to virtually all known physiological and pathological processes, such as cell differentiation and proliferation, developmental timing, neuronal asymmetry, apoptosis, insulin secretion, and various metabolic reactions.[1,2] In addition, the change of miRNA levels in many human diseases suggests that miRNA expression profiling could be used for defining clinical phenotypes, as well as potentially useful molecular diagnostic markers. However, accurately measuring miRNA levels has also posed numerous new challenges to the analytical technologies. Given the short length of the miRNAs with inherently different melting temperatures, their trace levels in the cell (typically <1% relative to the other cellular RNAs), and the highly similar sequences between miRNA family members,[2] the detection methods need to be extremely sensitive. In addition, they need to be specific to accurately measure the levels of specific analytes in small amounts of complex RNA sample.

At the present time, the majority of the microRNA detection relies on techniques like Northern blot[3−5] and reverse transcriptase-polymerase chain reaction (RT-PCR).[6] In the Northern blot method, the sample containing miRNA is run on an electrophoresis gel. Next, the miRNA is transferred to a nitrocellulose membrane, followed by soaking in a solution containing a fluorescent or radiolabeled oligonucleotide probe which is complementary to the target miRNA for hybridization to occur. These methods are time-consuming, have low throughput, and require a relatively large amount of RNA material. To avoid using radioactive isotopes and a large amount of total RNA, different methods have been developed on the basis of quantitative RT-PCR (qRT-PCR) as it combines the exceptional amplification power of PCR with quantitative detection of the amplified products during each reaction cycle. While RT-PCR can be used to quantitatively detect small amounts of miRNA, the requirement of short primers decreases the assay stringency. Additionally, the commercially available kits are expensive; the laboratory procedures require a long time for the assay and the use of an equipped laboratory with specialized and well-trained biologists and are not feasible for routine serum-based miRNA determination.

To enable detection of the extremely low concentration over a wide dynamic range in which miRNA is present in cells (<1% of total cell RNAs) and human serum (0 to 1 pM), we have integrated a highly selective biorecognition element, the RNA binding protein p19 from Carnation Italian ringspot virus (CIRV), with an extremely sensitive carbon nanotubes field-effect transistor (CNTs-FET) transducer for a label-free, fast, facile, and low cost nanobiosensor (Figure 1). This is the first report of a biosensor using p19 and CNTs-FET combination

**Received:** June 18, 2013
**Accepted:** August 2, 2013

   dx.doi.org/10.1021/ac4018346 | *Anal. Chem.* XXXX, XXX, XXX−XXX

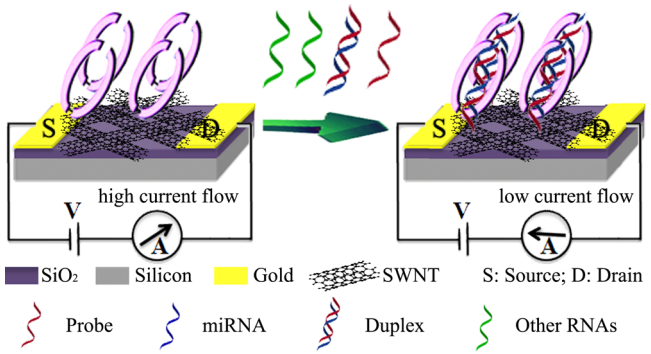


**Figure 1.** Schematic of miRNA detection principle by the p-19 functionalized CNTs-FET nanobiosensor.

for electronic detection of miRNA. The p19 is a 19 kDa protein expressed by plant viruses to function as a suppressor of the RNA silencing pathway and binds with high affinity only to double stranded/duplex RNA (dsRNA) in a size-specific and sequence-independent manner; i.e., it does not bind ssRNA, tRNA, rRNA, ssDNA, or dsDNA.[7,8] The p19 binding affinity is determined by the miRNA duplex region length. For example, it has the highest affinity for 21−23 nt dsRNA which progressively becomes weaker for 24−26 nt dsRNA and very low for 19 nt and smaller. Hybridization of a miRNA-specific probe to a single-stranded target miRNA creates dsRNA that tightly binds the p19 fusion protein. Binding of the dsRNA to the protein results in a change in conductance of the CNTs, and the amount of target miRNA in the sample is quantified by measuring the change in resistance from the *I*−*V* curve (Figure 1). miRNA-122a, a specific liver marker expressed in 70% of liver cells,[9] which has been linked with lipid metabolism, liver homeostasis,[10,11] and hepatitis C virus replication,[12] was studied as a model target. This nanobiosensor detected the target miRNA-122a from 1 aM to 10 fM in the presence of a million-fold excess of total RNA and other miRNA sequences. The 1 aM limit of detection is the best reported to date.

The nanobiosensor fabrication started with the construction of the CNTs-FET device using 3-aminopropyltriethoxysilane (APTES)-assisted assembly of CNTs from a 95% enriched semiconductive nanotubes ink (Nanointegris Inc., CA) across 3 $\mu$m spaced microfabricated interdigitated gold electrodes acting as source and drain on $Si/SiO_2$ (Supporting Information, Figure S1) followed by annealing in air at 250 °C for an hour. Although simple, the APTES-assisted technique produced FET devices with reproducible high density networks (Supporting Information, Figure S2) of starting resistances (3.2 ± 1.1 kΩ) and on−off ratios (2.58 ± 1.02). The CNTs-FET devices were next functionalized with p19 (New England BioLabs, MA) through the 1-pyrenebutanoic acid succinimidyl ester (PBASE), and finally, the naked/bare CNTs sites were treated with Tween 20 to block nonspecific adsorption.

The above fabrication steps were monitored by recording the current−voltage (*I*−*V*) characteristics of the device between +1 and −1 V after each step by a semiconductor parameter analyzer. As shown in Figure 2, the drive current in the CNTs-FET device at a given voltage decreased after modification by PBASE, p19, and Tween 20. The observed current decreases or resistance increases are in accordance with the literature and are attributed to $\pi-\pi$ stacking interaction between CNTs and pyrene in the case of PBASE and scattering potential generated

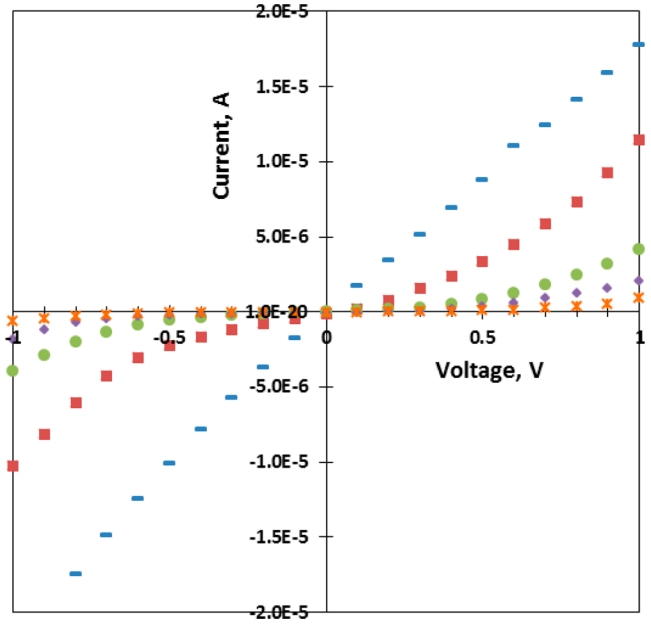


**Figure 2.** *I*−*V* characteristics of the biosensor at various stages of miRNA detection. (blue −) Bare CNTs; (pink ■) CNTs functionalized with PBASE; (green circle) after p19 immobilization; (purple ◆) after blocking unoccupied sites with Tween 20; (orange ∗) 10 $\mu$L of 10 fM miRNA-122a target + 1 $\mu$M miRNA-122a probe after 1 h incubation at 37 °C.

and/or electron donation from the molecules to the nanotubes in the case of p19 and Tween 20.[13]

Next, we evaluated the potential of p19-functionalized CNTs-FET as miRNA nanobiosensor. Ten femtomolar of synthetic miRNA-122a (5′-pUGG AGU GUG ACA AUG GUG UUU G-3′) was incubated with 1 $\mu$M of miRNA-122a−specific RNA probe and 5′-pAAC ACC AUU GUC ACA CUC CAU A-3′ (complementary to miRNA-122a with two-nucleotide 3′ extension[7,14]) at 22 and 37 °C for 1 h in pH 7.4, 10 mM phosphate buffer (PB) in a total volume of 100 $\mu$L followed by incubation of 10 $\mu$L of the reaction mixture with nanobiosensor for 1 h at room temperature, washing 5 times with 500 $\mu$L of PB buffer and measuring the *I*−*V* characteristics. As illustrated in Figure 2, the device current decreased (i.e., resistance increased) further, attributed to the accumulation of probe-target duplex of miRNA-122a bound to the p19 protein. The normalized resistance change calculated from the inverse of the slope of the linear range (+0.2 to −0.2 V) of the *I*−*V* curve was 2.22. In comparison, incubation with 1 $\mu$M of miRNA-122a target alone (positive control) produced a normalized resistance increase of only 0.015. Similarly, transistors in which CNTs were not modified with p19 but were treated with only Tween 20 to make the nanotubes hydrophilic when incubated with the probe and target mixture incubated at 37 °C for 1 h (negative controls) increased the normalized device resistance by 0.011. These results confirmed that the nanobiosensor response when incubated with the mixture of target miRNA with the probe was the result of p19 binding selectively to the hybridized duplex and thus the potential of the nanobiosensor as a specific, rapid, facile, and cost-effective analytical device for miRNA.

The effect of temperature on nucleic acid hybridization is well-established. Higher temperature leads to uncoiling of nucleic acid strands making the probe and target strands more


dx.doi.org/10.1021/ac4018346 | *Anal. Chem.* XXXX, XXX, XXX−XXX

accessible to one another, leading to improved hybridization efficiency and better specificity due to difference in the thermal stability of perfectly matched and mismatched duplexes.[14] A comparison of the sensor performance at two temperatures showed that hybridization at 37 °C generated an enhanced signal over hybridization at 22 °C (Supporting Information, Table S1), and 37 °C was selected for further studies.

After establishing the feasibility of detecting miRNA by the developed biosensor, we investigated its potential for quantitative detection, sensitivity, dynamic range, and limit of detection. Increasing concentrations (1 aM to 10 fM) of synthetic miRNA-122a were incubated with 1 $\mu$M of miRNA-122a–specific RNA probe in a 100 $\mu$L total volume of PB at 37 °C for 1 h followed by incubation of 10 $\mu$L of the reaction mixture with nanobiosensor for 1 h at room temperature, washing 5 times with 500 $\mu$L of PB buffer and measuring the $I$–$V$ characteristics. Figure 3 shows the normalized response of

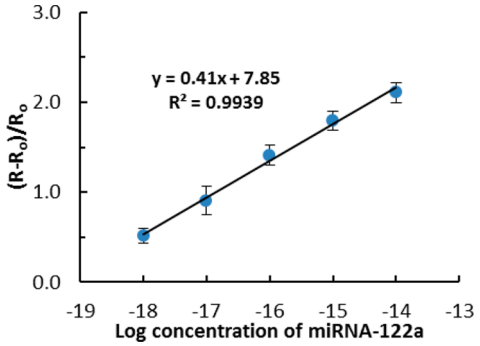


**Figure 3.** Nanobiosensor calibration for miRNA-122a in buffer. The data points are averages of measurements from 7 independent biosensors, and error bars represent ±1 standard deviation.

the nanobiosensor [$(R - R_0)/R_0$, where $R$ is the resistance after incubation with dsRNA and $R_0$ is the resistance after blocking of unoccupied sites with Tween 20, determined from the inverse of the slope of the $I$–$V$ curve from +0.2 to −0.2 V] as a function of log of miRNA-122a concentration. As shown in the figure, the response was linear over the range of 1 aM to 10 fM and a regression equation of $y = 0.41x + 7.85$ ($R^2 = 0.9939$) was obtained, where $y$ is the relative change in resistance ($(R - R_0)/R_0$) and $x$ is the logarithmic concentration of miRNA-122a. This detection limit is 10- to 100-fold better than other recently reported p19-based assays and sensors, some of which used labels including radioactive $^{32}$P[7,15–17] and 1000-fold better than the peptide nucleic acid probe functionalized silicon nanowire FET.[18]

For a real-world application, the nanobiosensor should be able to differentiate the target from other miRNAs and detect the target in a complex mixture. To evaluate the specificity, nanobiosensor response to the reaction mixture of 1 $\mu$M of miRNA-122a probe and 10 fM miRNA-21 (5′-pUAG CUU AUC AGA CUG AUG UUG A-3′) or miRNA-32 (5′-pUAU UGC ACA UUA CUA AGU UGC A-3′) after incubation at 37 °C for 1 h was measured. As shown in Figure 4, both miRNAs generated an insignificant resistance change when compared to the perfect match target (miRNA-122a). Additionally, to investigate the potential of detecting the extremely low concentration of target miRNA in the presence of other nucleic acids, a calibration plot of the biosensor response as a function of miRNA-122a concentration in the presence of 10 $\mu$g of total yeast RNA was generated following the protocol

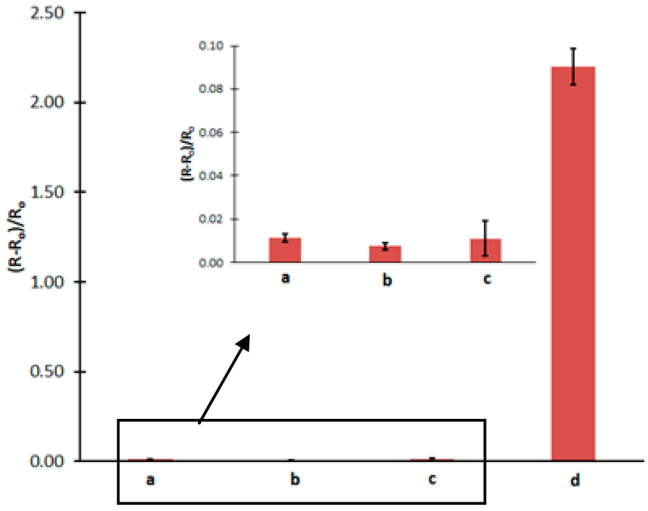


**Figure 4.** Nanobiosensor selectivity. Responses of nanobiosensors to reaction mixtures of 1 $\mu$M miRNA-122a probe with 10 fM miRNA-21 (a), 10 fM miRNA-32 (b), 10 $\mu$g of total yeast RNA (without miRNA-122a target) (c), and 10 fM miRNA-122a (d) after incubation for 1 h at 37 °C. Inset shows a magnified view. The data points are averages of measurements from 10 independent biosensors, and error bars represent ±1 standard deviation.

described previously ($I$–$V$ characteristic curves shown in Supporting Information, Figure S3). As shown in Figure 5,

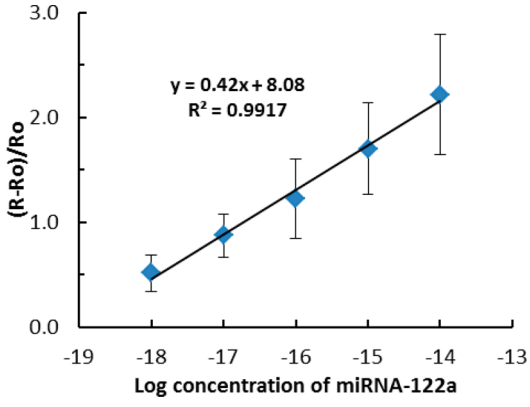


**Figure 5.** Nanobiosensor calibration for miRNA-122a in the presence of 10 $\mu$g of total yeast RNA. The data points are averages of measurements from 10 independent biosensors, and error bars represent ±1 standard deviation.

the calibration plot was linear over the range of 1 aM to 10 fM and had a regression equation of $y = 0.42x + 8.08$ ($R^2 = 0.9917$). These are very similar to the analytical characteristics for the miRNA-122a analysis in buffer, showing the ability of the developed sensor to detect the target even in a large excess of other nucleic acids.

In conclusion, we have developed a label-free nanobiosensor for fast, facile, inexpensive, highly specific, and ultrasensitive quantitative determination of miRNA in nucleic acid samples. The biosensor takes advantage of the high affinity and specificity of CIRV p19 protein for 21–23 nucleotide duplex RNA and the high sensitivity of CNTs-FET to quantitatively measure as low as 1 aM to up to 10 fM of probe-specific target miRNA selectively and in a million-fold excess of other nucleic acids. Importantly, the 1 aM detection limit was achieved without employing any amplification techniques and is well


dx.doi.org/10.1021/ac4018346 | Anal. Chem. XXXX, XXX, XXX–XXX

below the levels of interest in biological and medical diagnostics even after diluting the sample which can further reduce any potential matrix interference. Moreover, the base mismatch discrimination can be achieved through selection of hybridization conditions, as is done in commonly employed nucleic acid detection methods. For example, by performing hybridization in a 50% formamide solution, Qavi and Bailey successfully achieved discrimination between microRNAs let-7b and let-7c, which differ by a single-base change at position 17.[19] A similar strategy can be employed in our platform. The methodology developed in this work can be applied for fabricating an array of sensors on a single silicon substrate for multiplex sensing for miRNA expression profiling. Furthermore, the developed sensors are based on silicon microelectronics that are cheap and readily scalable to mass scale manufacturing.

## ■ ASSOCIATED CONTENT

### Supporting Information

Details of device fabrication, sensing protocol, I−V data, and SEM image of CNT networks. This material is available free of charge via the Internet at http://pubs.acs.org.

## ■ AUTHOR INFORMATION

### Corresponding Author

*E-mail: adani@engr.ucr.edu.

### Author Contributions

†P.R. and Y.G. contributed equally.

### Notes

The authors declare no competing financial interest.

## ■ ACKNOWLEDGMENTS

We acknowledge the financial support of Nanosense Inc. and the U.S. Department of Agriculture.

## ■ REFERENCES

(1) Carthew, R. W. *Curr. Opin. Genet. Dev.* **2006**, *16*, 203−208.
(2) Zamore, P. D.; Haley, B. *Science* **2005**, *309*, 1519−1524.
(3) Valoczi, A.; Hornyik, C.; Varga, N.; Burgyan, J.; Kauppinen, S.; Havelda, Z. *Nucleic Acids Res.* **2004**, *32*, e175.
(4) Kloosterman, W. P.; Wienholds, E.; de Bruijn, E.; Kauppinen, S.; Plasterk, R. H. *Nat. Methods* **2006**, *3*, 27−29.
(5) Varallyay, E.; Burgyan, J.; Havelda, Z. *Nat. Protoc.* **2008**, *3*, 190−196.
(6) Shi, R.; Chiang, V. L. *Biotechniques* **2005**, *39*, 519−525.
(7) Jin, J.; Cid, M.; Poole, C. B.; McReynolds, L. A. *Biotechniques* **2010**, *48*, 17−23.
(8) Vargason, J. M.; Szittya, G.; Burgyan, J.; Hall, T. M. T. *Cell* **2003**, *115*, 799−811.
(9) Girard, M.; Jacquemin, E.; Munnich, A.; Lyonnet, S.; Henrion-Caude, A. *J. Hepatol.* **2008**, *48*, 648−656.
(10) Esau, C.; Davis, S.; Murray, S. F.; Yu, X. X.; Pandey, S. K.; Pear, M.; Watts, L.; Booten, S. L.; Graham, M. *Cell Metab.* **2006**, *3*, 87−98.
(11) Chang, J.; Guo, J. T.; Jiang, D.; Guo, H.; Taylor, J. M.; Block, T. M. *J. Virol.* **2008**, *82*, 8215−8223.
(12) Jopling, C. L.; Norman, K. L.; Sarnow, P. *Cold Spring Harbor Symp. Quant. Biol.* **2006**, *71*, 369−376.
(13) Tlili, C.; Cella, L. N.; Myung, N. V.; Sheety, V.; Mulchandani, A. *Analyst* **2010**, *135*, 2637−2642.
(14) Wallace, R. B.; Shaffer, J.; Murphy, R. F.; Bonner, J.; Hirose, T.; Itakura, K. *Nucleic Acids Res.* **1979**, *6*, 3543−3557.
(15) Wanunu, M.; Dadosh, T.; Ray, V.; Jin, J.; McReynolds, L.; Drndic, M. *Nat. Nanotechnol.* **2010**, *5*, 807−814.
(16) Labib, M.; Khan, N.; Ghobadloo, M. S.; Cheng, J.; Pezacki, J. P.; Berezovski, M. V. *J. Am. Chem. Soc.* **2013**, *135*, 3027−3038.
(17) Khan, N.; Cheng, J.; Pezacki, J. P.; Berezovski, M. V. *Anal. Chem.* **2011**, *83*, 6196−6201.
(18) Zhang, G. J.; Chua, J. H.; Chee, R. E.; Agarwal, A.; Wong, S. M. *Biosens. Bioelectron.* **2009**, *24*, 2504−2508.
(19) Qavi, A. J.; Bailey, R. C. *Angew. Chem., Int. Ed.* **2010**, *49*, 4608−4611.


dx.doi.org/10.1021/ac4018346 | *Anal. Chem.* XXXX, XXX, XXX−XXX